REPORT DOCUMENTATION PAGE

Form Approved
OMB No. 0704-0188

PLEASE DO NOT RETURN YOUR FORM TO THE ABOVE ORGANIZATION.

1. REPORT DATE *(DD-MM-YYYY)*	2. REPORT TYPE	3. DATES COVERED *(From - To)*
05-08-2009	Conference Proceeding	

4. TITLE AND SUBTITLE
Microbiological and Corrosivity Characterizations of Biodiesels and Advanced Diesel Fuels

5a. CONTRACT NUMBER

5b. GRANT NUMBER

5c. PROGRAM ELEMENT NUMBER
0602123N

6. AUTHOR(S)
Jason S. Lee, Richard I. Ray, Brenda J. Little

5d. PROJECT NUMBER

5e. TASK NUMBER

5f. WORK UNIT NUMBER
73-9611-08-5

7. PERFORMING ORGANIZATION NAME(S) AND ADDRESS(ES)
Naval Research Laboratory
Oceanography Division
Stennis Space Center, MS 39529-5004

8. PERFORMING ORGANIZATION REPORT NUMBER
NRL/PP/7330-08-9020

9. SPONSORING/MONITORING AGENCY NAME(S) AND ADDRESS(ES)
Office of Naval Research
800 N. Quincy St.
Arlington, VA 22217-5660

10. SPONSOR/MONITOR'S ACRONYM(S)
ONR

11. SPONSOR/MONITOR'S REPORT NUMBER(S)

12. DISTRIBUTION/AVAILABILITY STATEMENT
Approved for public release, distribution is unlimited.

13. SUPPLEMENTARY NOTES

14. ABSTRACT

Experiments have been designed to evaluate the nature and extent of microbial contamination and the potential for microbiologically influenced corrosion in biodiesel (B100), ultra-low sulfur diesel (ULSD) and mixtures of the two (B5 and B20). In experiments with additions of distilled water, B100 has the highest propensity for biofouling while the highest corrosion rates were measured in ultra-low-sulfur diesel.

15. SUBJECT TERMS
corrosion, diesel, biodiesel, biofouling, MIC

16. SECURITY CLASSIFICATION OF:			17. LIMITATION OF ABSTRACT	18. NUMBER OF PAGES	19a. NAME OF RESPONSIBLE PERSON
a. REPORT	b. ABSTRACT	c. THIS PAGE			Jason Lee
Unclassified	Unclassified	Unclassified	UL	22	19b. TELEPHONE NUMBER *(Include area code)* 228-688-4494

Published 3/22/2009

Paper No.
09529

NACE INTERNATIONAL CORROSION 2009 CONFERENCE & EXPO

MICROBIOLOGICAL AND CORROSIVITY CHARACTERIZATIONS OF BIODIESELS AND ADVANCED DIESEL FUELS

Jason S. Lee*, Richard I. Ray*, Brenda J. Little**
Naval Research Laboratory
Codes 7332*/7303**
Stennis Space Center, MS 39529

ABSTRACT

Experiments were designed to evaluate the nature and extent of microbial contamination and the potential for microbiologically influenced corrosion in biodiesel (B100), ultra-low sulfur diesel (ULSD) and mixtures of the two (B5 and B20). In experiments with additions of distilled water, B100 had the highest propensity for biofouling while the highest corrosion rates were measured in ultra-low-sulfur diesel.

Keywords: corrosion, diesel, biodiesel, biofouling, MIC

INTRODUCTION

Microbial contamination of hydrocarbon fuels has been recognized as a problem for over 40 years. Microbial contamination of hydrocarbon fuels is the main cause of 1) clogging of fuel lines and filters, 2) product deterioration and 3) corrosion of metals during hydrocarbon extraction, production, distribution and storage.[1] The following mechanisms for microbiologically influenced corrosion (MIC) in fuel/water systems were elucidated by Videla *et al.*[1] 1) local increase in proton concentration derived from organic acidic metabolites, 2) increase of the oxidizing characteristics of the medium favoring pitting attack, 3) metabolite production decreasing the surface energy of the interface passive film/electrolyte, 4) microbial adhesion enhancing metal dissolution and 5) microbial uptake of fuel additives, including corrosion inhibitors.

Requirements for microbial growth are water and nutrients. In addition to carbon, all organisms require nitrogen, phosphorus and sulfur and other trace elements for growth. The major limitation for microbial activity in fuels is the presence of water.[2] The volume of water required for microbial growth is extremely small and water is a product of the microbial mineralization of hydrocarbons. It is possible for microbial mineralization of fuel to generate a water phase for further proliferation. For example, *Cladosporium resinae* grew in 80 mg water per liter of kerosene and after four weeks incubation, the concentration of water increased more than ten-fold.[3] The relationship between microorganisms, fuel

and water is complicated. In general, acrobic microorganisms (fungi and aerobic bacteria) grow at the fuel water interfacc and anaerobic bacteria (e.g., sulfate-reducing bacteria) grow in oxygcn-free areas e.g., at the bottom of a storage tank. Nutrients are dissolved from the fuel into the water. In a frecstanding clean tank most of the water is water of condensation accumulated at the bottom of the tank and amounting to a few percent of the volume of the tank. Water in fuel can also form an emulsion. Most water-in-oil emulsions are unstable and over time the water drops to the bottom of the tank. Under some circumstances bacteria and fungi can produce surfactants, causing the formation of stable water-in-oil emulsions.

The susceptibility of hydrocarbons to aerobic and anaerobic biodegradation is well known and the subject has been reviewed.[4-15] It is clear that the oxidation of many different types of hydrocarbons can be coupled with the reduction of a variety of electron acceptors in addition to oxygen and that CO_2 is the resulting endproduct. It is also clear that anaerobes can couple their metabolism in syntrophic associations that ultimately allow for the conversion of the petroleum components to methane.[9-27]

McNamara *et al.*[28] demonstrated that the dominant microorganisms contaminating jet fuels changed over the years with changes in formulations, refinery practices, chemical compositions and biocides. With the introduction of ultra low-sulfur diesels (ULSD) (<15 ppm S) and biodiesel (BD), new problems may be encountered.[29] Londry and Suflita[30] found that thiophenes, thiols, thiophenic acids and aromatic sulfides found in high sulfur diesels could inhibit a variety of metabolic processes in anaerobic cultures cnriched from an oily sludge. In addition the desulfurization processes may make low sulfur diesel more biodcgradable by producing biodegradable components.[31] Biodiesels are inherently more susceptible to microbial decay that typical hydrocarbon fuels since methyl esters are hydrolyzed with ease under aerobic or anaerobic conditions. When microorganisms hydrolyze biodiesel fuels they produce fatty acids. Knothe and Steidley[32] suggested that the free fatty acids can restore lubricity to ULSD. It follows that there may be additional problems related to microbial contamination.

Experiments were designed to evaluate the nature and extent of microbial contamination and the potential for microbiologically influenced corrosion in BD, ULSD and mixtures of the two. The main objectives of this work were: (1) characterize the corrosion and electrochemical behavior of storage and fuel tank alloys in the presence of diesel mixtures over time; (2) determine the microflora and chemistry of as-received diesel mixtures as a function of BD content and storage time.

MATERIALS AND METHODS

Uncoated aluminum, carbon steel, and stainless steel alloys were exposed to a range of diesel fuels and water mixtures. Diescl mixtures included various proportions of ULSD and BD. Red dyed high-sulfur (> 150 ppm S) diesel fuel (designated L100) was used as a control. Distilled water was added to simulatc condensate. Corrosion behavior was examined by electrochemical techniques. Corrosion products, surface microflora, and corrosion morphology were characterized by environmental scanning electron and optical microscopy. Bacterial and fungal species were identified using molecular techniques. Full specification analysis was conducted on the pre-test fuels and a more detailed analysis conducted on both the prc- and post-test fuel mixtures.

Metal Coupons

Carbon steel UNS C10200, stainless steel UNS S30403, and aluminum alloy UNS A95052 were sclected as representative fuel tank alloys (Tables 1). Metal coupons of each alloy were fabricated with

dimensions of 5/8" (1.5875 cm) diameter and 1/8" (0.3175 mm) thick.* A wire was attached to the back side of each coupon with conductive epoxy and carbon tape to achieve electrical connection. Coupons were individually mounted in epoxy† to electrically isolate the wire connection and to establish an exposed area of 2 cm^2 as shown. Each coupon was wet-polished to a 600 grit finish, sonicated in soapy water, rinsed with acetone and blown dry with nitrogen gas.

Fuel/Water Mixtures

Five diesel fuel mixtures were examined:

- ULSD - 100% ULSD - (clear)
- L100 - 100% L100 – (red-dyed)
- B100 - 100% BD - soybean feedstock (yellow color)
- B5 – 5% BD / 95% ULSD Blend (% by volume)
- B20 – 20% BD / 80% ULSD Blend (% by volume)

The first three diesel fuels (ULSD, L100, B100) were purchased locally. B5 and B20 were mixed under laboratory conditions from the ULSD and B100 supplies.

For electrochemical experiments, 900 mL of distilled water was mixed with 900 mL of fuel mixture (1:1) in a 2L crystallization dish with a watch glass cover. No further method was employed to seal the containers. This procedure was repeated for each fuel mixture twice to give a total of ten exposure containers.

In addition to the native microbiology in the fuel samples, an inoculum was prepared from fuel tank sludge. Each test vessel was inoculated with water from a three year old fuel source in the following manner: 100 mL of water was collected from a 500 mL LSD/distilled water mixture that had been sealed in a jar for three years. Approximately, 100 mL of distilled water was added each day until the total volume of water was increased to 2 L. At the onset of the experiment, 10 mL of the inoculum was added to each fuel water mixture.

Laboratory temperature was maintained at 23°C with fluorescent lighting for 8 hours a day. No attempt was made to sterilize glassware, coupons, wires, or plastic mounts prior to introduction of fuel/water mixtures. Total exposure time was 6 months.

Microbiology Identification

At the onset of the experiment, 900 mL of each of the three unmixed fuels ULSD, B100, and L100 were combined with 900 mL of distilled water, placed on a shaker at 60 rpm to encourage mixing and native fuel microorganisms to enter the water layer (Figure 1). After 2 weeks, the water and fuel were separated using a separation funnel. Each of the water samples, along with 900 mL of the inoculum (described above) was sent to a commercial laboratory‡ for microflora genetic determination by denaturing gradient gel electrophoresis (DGGE).[33] For bacteria, the DDGE technique separated the amplified 16S rRNA genes, whercas for fungi the 28S rRNA gene was used to form banding patterns. Banding patterns and their relative intensities lead to a measure of the differences of microflora communities. The most intense bands were excised and sequenced to determinc the identity of the corresponding microorganism.[34] At the conclusion of the 6-month exposure, this method was repeated for each water sample from the 10 containers.

---

* Metal Samples, Munford, AL
† Epothin™, Buehler Ltd., Lake Bluff, IL
‡ Microbial Insights, Rockford, TN

Fuel and Water Chemistry

One liter of each of the unmixed fuels ULSD, B100 and L100 were sent to a government laboratory[§] prior to experiment onset. Specification testing was performed on all three fuels using the Navy's F-76 specification, MIL-DTL-16884. Gas chromatography-mass spectrometry (GC-MS) analysis was conducted on both pre- and post-test fuels including ULSD, L100, B5, B20 and B100. Post-test samples were analyzed by temperature-programmed GC-MS with the following operational conditions:

- 1 µL diluted in 1 mL methylene chloride, 1 µL injected with a 1:10 split
- Column - HP-5, 30m, 0.25mm ID, 0.25 µm df, flow 1.5 mL/min
- Oven temperature - 50 °C to 290 °C at 10 °C/min
- Mass-selective detector scanned from 30-300 m/z

The pH of each water layer was measured pre- and post-exposure.

Electrochemical Methods

Three epoxy mounted coupons of each alloy were used to each of the five fuel/water combinations. Coupons were vertically orientated in the exposure vessels at the fuel water interfaces held in place by a plastic mount. Aluminum and stainless steel alloy coupons were exposed in the same container, while carbon steel coupons were exposed separately (10 total containers). A mercury/mercury sulfate electrode and a 4 cm^2 platinum-niobium mesh were used as reference and counter electrodes, respectively in a standard three-electrode electrochemical setup. A Luggin probe filled with the saturated potassium sulfate (K_2SO_4) solution was employed to decrease the effect of voltage drop.

A computer-controllcd potentiostat[**] was employed for all electrochemical measurements. For each measurement, the Luggin probe was positioned at the fuel/water interface to within 5 mm of the coupon surface. Solution resistance (R_s) between the coupon and the Luggin probe was determined by clectrochemical impedance spectroscopy (EIS). The measured impedance at the highest frequcncy with a phase angle greater than -5 degrees was recorded as R_s. All distilled water/fuel mixtures had significant R_s values within the range of 10^4 to 10^7 ohm-cm^2. Corrosion potential (E_{corr}) was recorded for each coupon vs. the reference electrode. Polarization resistance (R_p) was determined by employing the linear polarization resistance technique (LPR).[35] Current was recorded as the potential of each coupon was scanned from -10 mV to +10 mV vs. E_{corr}. A slow scan rate of 0.16 mV/s was used during LPR to compensate for the lack of charge carriers in solution. R_p was determined from the Ohm's Law relationship:

$$V = I \times (R_p + R_s) \tag{1}$$

where V is potential and I is current. Solving for R_p results in,

$$R_p = \frac{V}{I} - R_S \tag{2}$$

where the slope of the LPR measurement (V/I) (determined by least squares fit) less the EIS measured R_s gives R_p. A commercially available program[††] was used to automate the determination of R_p. The inverse ($1/R_p$) is proportional to the instantaneous corrosion rate. The term 'instantaneous' is used here to distinguish it from a cumulative corrosion rate determination such as weight loss. LPR gives the

[§] NAVAIR Pax River - Naval Fuels and Lubricants CFT
[**] Model PC4, Gamry Instruments, Warminster, PA
[††] Echem Analyst ver5.5, Gamry Instruments, Warminster, PA

corrosion rate at the instant in time of the measurement; it provides no information of corrosion that has occurred previously. R_p, R_s, and E_{corr} were measured every one to two weeks for all exposed samples and averaged for each triplicate set of alloy/fuel mixture exposures.

Post-Exposure Surface Examination

After 6 month exposure period, each coupon was removed from its container by lifting through the fuel layer. Coupons were imaged using a macro digital camera.[‡‡]

RESULTS AND DISCUSSION

Fuel/Water Chemistries and Microflora

pH

The pH of distilled water was 5.75 prior to addition to fuels. After 6 months exposure to the different fuels and including either C10200 alone or S30403 and A95052 together, the pH of the water layers were re-measured with results shown in Table 2. For exposures with C10200, the highest pH value was 6.64 for ULSD, the lowest was 3.41 for L100 with BD containing fuels having intermediate values. Increasing BD content corresponded with lower pH values. For exposures with the stainless steel and aluminum alloy, pH values followed the same basic trends as in the carbon steel exposures. The notable exceptions were the ULSD exposure with a pH = 4.98 (C10200/ULSD pH = 6.64) and the B20 exposure with a pH = 5.21 (higher than B5 with pH = 4.93).

Visual Observations

The container with ULSD and C10200 had visible dark orange precipitates collected at the bottom of the water layer, presumably iron oxide/hydroxide corrosion products (Figure 2). B5, B20, and B100 containers all showed evidence of biofouling at the fuel/water interface and in the water layer itself in the form of colored masses. Figure 3 shows an example of a fungal mass growing in the water layer on one of the plastic electrode mounts with B100 after 6 months. Figure 3 also shows the color change in B100 over the 6 month-period exposure. Initial color was a dark yellow (Figure 1) while the exposed B100 turned to a bright green. Over the same 6 month period, B100 stored in an opaque sealed container with no added water and no inoculum retained the original yellow color.

Fuel Specifications

Table 3 lists the U.S. Navy's F-76 specification limits and the corresponding measured values of the pre-exposure fuels ULSD, L100, and B100. Data are presented for completeness and will not be discussed in detail, only specific data highlighted. Measured Acid Number provides insight into the measured pH values of water layers exposed to each fuel (or mixture) for 6 months. L100 had the highest acid number (1.95) corresponding to the lowest water layer pH values measured (Table 2). ULSD had the lowest Acid Number (0.03) and B100 had an intermediate value of 0.26 corresponding to the highest and intermediate pH values measured for ULSD and B100/ULSD mixtures, respectively. Sulfur level in L100 was determined to be 1,273 ppm in comparison to B100 and ULSD which had values of 3 and 2, respectively.

[‡‡] Nikon Model S-700

GC-MS

GC-MS examination of fuels provided fatty acid methyl ester (FAME) content with regards to carbon chain length denoted by the convention C# (number of carbons in chain). Pre-exposure B100 fuel was composed of C17 and C19 FAME. After 6 months exposure to C10200 and S30403+A95052, C21, C23, and C25 FAME were detected in addition to C17 and C19. Also, the same FAME content (C17+C19+C21+C23+C25) was measured from a sample of B100 under identical conditions but without metal coupon inclusion. These results indicate that metal inclusion was not necessary for alteration of FAME chemistry. The change in FAME chemistry may have resulted in the color change from yellow to green as seen in Figures 1 and 3, respectively. The color change along with the formation of higher C number FAME suggests the possibility of polymerization. Whether the polymerization was caused microorganisms, light, evaporation, or water uptake is unknown.

All L100 fuels had C17+C19 FAME content indicating a biodiesel/petrodiesel blended fuel. All ULSD fuels (pre- and post-exposure) had 0% FAME content indicating no biodiesel blending. B20 and B5 fuels contained C17+ C19 FAME, while no C21+C23+C25 FAME were detected.

In addition, much higher levels (order-of-magnitude) of volatile components, including ethylbenzene and xylenes, were detected in pre-exposure L100 than ULSD. Significant decreases in volatile components were measured in post-exposure L100 and ULSD, which is likely due to the exposure containers not being firmly sealed.

Microflora

Bacterial and fungal genetic sequencing was performed on water layers exposed for 2 weeks to the pre-exposure test fuels ULSD, L100 and, B100. The inoculum was also sequenced. Table 4 shows the dominate microorganisms in each sample and the corresponding band pattern from the DGGE. All samples had evidence of both bacterial and fungal species except L100, where fungal species could not be cultured.

After the 6 month exposure period, the water layers from each container were also sequenced again (Table 5). In regards to bacterial population, *Sphingomonas* spp. was found in each sample that could be cultured. From Table 4, *Sphingomonas* spp. was native to B100 and ULSD. In regards to fungal species, *Aureobasidium* and *Paecilomyces* spp. were sequenced from BD-containing fuels. The fungal species *Rhodotorula* was the only microorganism from the inoculum sequenced after the 6 month exposure and was found in B20 with C10200. These results indicate that the native microorganisms in the original fuels dominated over the microorganisms in the inoculum and species diversity decreased over exposure time.

Electrochemical Behavior

Carbon Steel

E_{corr} ($V_{Hg/HgSO_4}$) and $1/R_p$ (instantaneous corrosion rate [ohm-cm^{-2}]) trends were recorded and over the 6 month exposure period for each alloy/fuel/water exposures. Each data point represents the average valuc of the 3 coupons of the same alloy. Figure 4 shows E_{corr} and 1/Rp trends for C10200 exposed to each of the 5 fuel/water mixtures. Exposure to ULSD exhibited the highest corrosion rates (10^{-3} ohm-cm^{-2}) (2 orders-of-magnitude higher than L100) and the lowest E_{corr} values (-1.0 $V_{Hg/HgSO_4}$) indicating the highest propensity for corrosion. C10200 in L100 had the second highest corrosion rate with intermittent spikes of an order-of-magnitude increase at days 29 and 56. E_{corr} started out at ~0.0 V but by day 150, had significantly dropped to -0.8 $V_{Hg/HgSO_4}$. In general, BD-containing fuels had the lowest corrosion rates -

($>10^{-7}$ ohm-cm^{-2}) and stable E_{corr} values ranging from 0.0 to -0.3 $V_{Hg/HgSO_4}$ over the entire 6 month exposure.

Stainless Steel

Figure 5 shows the E_{corr} and $1/R_p$ trends for S30403 exposed to each of the 5 fuel/water mixtures. All E_{corr} values ranged from 0.15 to -0.3 $V_{Hg/HgSO_4}$ with L100 and ULSD having the highest and lowest values, respectively. This E_{corr} range (0.45 V) was much smaller than the corresponding range for C10200 (1.0 V). S30403 exposed to BD-containing fuels exhibited the lowest corrosion rates with values (10^{-7} ohm-cm^{-2}) comparable to C10200 exposures. However, corrosion rates in B100 did increase to 10^{-6} ohm-cm^{-2} after 6 months corresponding to the values measured in ULSD and L100.

Aluminum Alloy

Figure 6 indicates the E_{corr} and $1/R_p$ trends for A95052 exposed to each of the 5 fuel/water mixtures. All E_{corr} values ranged from -0.5 to -1.25 $V_{Hg/HgSO_4}$, a much larger range than the S30403 exposures. E_{corr} for the L100 exposure dipped to -1.25 $V_{Hg/HgSO_4}$ in the first 7 days in comparison to the B100 exposure which rose to -0.7 $V_{Hg/HgSO_4}$. After 30 days, the L100 exposure had increased to -0.7, the same level as B100. B5, B20 and ULSD exposures all exhibited E_{corr} trends that increased by ~0.2 V over the 6 month period. In contrast, after the initial increase, L100 and B100 E_{corr} trends decreased by ~0.1V over the 6 month exposure period. E_{corr} trends coincided with increased corrosion rates for L100 and B100 over time and decreased corrosion rates for B5, B20, and ULSD exposures. L100 exposure corrosion rates increased from 10^{-6} ohm-cm^{-2} to near 10^{-4} ohm-cm^{-2} over the 6 month period with the next highest corrosion rate being the B100 exposure which was 2 orders-of-magnitude lower.

Macroscopic Surface Examination

After 4 days, an orange corrosion was visible on the C10200 coupons exposed to ULSD and distilled water below the fuel/water interface (Figure 7). In comparison, C10200 exposed to B100 only had a discoloration at the fuel/water interface (Figure 7). Corrosion products were not observed on the other C10200 fuel/water exposures or any of the S30403 or A95052 coupons.

After the 6 month exposure period, samples were removed from their respective containers and digitally photographed. Figure 8 displays the conditions of C10200 exposed to distilled water and the 5 different fuels: ULSD, L100, B5, B20, and B100. Exposure to ULSD resulted in large amounts of dark orange corrosion products at and below the fuel/water line. Exposure to L100 resulted in a thick dark red (almost black) deposit at the fuel/water interface. In addition, a thinner dark deposit on the area exposed to water was also observed with a rough texture either from an underlying corrosion product or the deposit itself. Exposure to B5, B20, B100 did not result in a visible corrosion since polishing marks were still imaged on the C10200 surfaces. However, debris was observed on the surfaces exposed to BD containing fuels below the fuel layer. The debris is believed to be biofouling which was also observed over the entire plane of the fuel/water interface.

In contrast to C10200, S30403 (Figure 9) and A95052 (Figure 10) did not show any visible signs of corrosion products and retained their respective polishing marks. For both S30403 and A95052, exposure to L100 resulted in a discoloration line at the fuel water interface and debris below it. A thick dark red deposit seen with C10200 (Figure 8) was not observed. Exposures to ULSD, B5, B20, and B100 resulted in varying amounts of debris at and below the fuel/water interface. In some instances (*e.g.*, A95052/ULSD, Figure 10) a clear mass was observed along the fuel/water interface.

ONGOING AND FUTURE WORK

One technical issue that is yet unresolved is the imaging of the coupon surfaces in an environmental scanning electron microscope (ESEM). At issue is the fuel layer through which the coupons are extracted through at the end of the experiment, fully coating the surface with a thin layer of fuel. If the fuel film is not removed prior to placement in the ESEM, fuel evaporation occurs as the vacuum is increased. The evaporated fuel coats the entire inside of the ESEM, including the optics making it impossible to image the surface. Removal of the fuel layer, by dissolving in organic solvents such as xylenes and acetone, removes the fuel layer but also destroys a large portion of biofilm accumulation. Different graded rinses are being explored in addition to removing most the fuel prior to extraction. While removing the bulk of the fuel is trivial, removing the last surface film over the water layer in much more complicated. At this time, the most promising method is brushing a highly absorbent cloth across the water surface and immediately extracting the sample.

Future work includes the aforementioned ESEM imaging of biofilms in addition to resulting corrosion products. Corroded surfaces will also be cleaned and the resultant corrosion morphology will be examined and compared with electrochemical measurements.

CONCLUSIONS

The approximately 1 Volt difference in measured E_{corr} values across the different exposure conditions for C10200 clearly demonstrates the differences in material/fuel mixture interactions for the different fuels: ULSD, L100, B100, B5, and B20. In regards to corrosion rates: 1) C10200/ULSD - had the highest electrochemically measured corrosion rate in this experiment, 2) S30403 exhibited passive behavior in all fuel/water mixtures, 3) A95052 exhibited its highest corrosion rates in ULSD followed by B100, otherwise passive behavior was observed, and 4) alloy exposures to B5, B20, B100 indicated the lowest corrosion rates for all materials. Visible biofouling was observed in BD mixtures. Overall, B100 had the highest propensity for biofouling while the highest corrosion rates were measured in ULSD exposures.

ACKNOWLEDGEMENTS

This work was supported by Dr. David Shifler at the Office of Naval Research (ONR Code 332) under award N0001408WX20857. The authors would also like to acknowledge S. Williams (Naval Fuels and Lubes CFT), K. J. Johnson, R. E. Morris, and M. H. Hammond (NRL Code 6181), and B. C. Giordano (Nova Research) for the work involving fuel chemical characterization. NRL Publication Number PP/7330/08/9020.

REFERENCES

1. H. A. Videla, P. S. Guiamet, S. DoValle, E. H. Reinoso, "Effects of fungal and bacterial contaminants of kerosene fuels on the corrosion of storage and distribution systems," CORROSION / 88, Paper no. 91 (Houston, TX: NACE International, 1988).

2. R. J. Watkinson, "Hydrocarbon degradation," in Microbial Problems and Corrosion in Oil and Oil Products Storage (London: The Institute of Petroleum, 1984), p. 50-56.

3. K. Bosecker, "Deterioration of hydrocarbons," in Microbiologically Influenced Corrosion of Materials, eds. E. Heitz, H. C. Flemming and W. Sands (Berlin: Springer-Verlag, 1996), p. 439-444.

4. H. R. Beller, "Metabolic indicators for detecting in situ anaerobic alkylbenzene degradation," Biodegradation 11, 2-3 (2000) p. 125-139.

5. J. Heider, "Adding handles to unhandy substrates: anaerobic hydrocarbon activation mechanisms," Curr Opin Chem Biol 11, 2 (2007) p. 188-194.

6. J. Heider, A. M. Spormann, H. R. Beller, F. Widdel, "Anaerobic bacterial metabolism of hydrocarbons," FEMS Microbiol Rev 22, 5 (1999) p. 459-473.

7. A. M. Spormann, F. Widdel, "Metabolism of alkylbenzenes, alkanes and other hydrocarbons in anaerobic bacteria," Biodegradation 11, 2-3 (2000) p. 85-105.

8. M. D. Zwolinski, R. F. Harris, W. J. Hickey, "Microbial consortia involved in the anaerobic degradation of hydrocarbons." " Biodegradation 11, 2-3 (2000) p. 141-158.

9. M. Boll, G. Fuchs, J. Heider, "Anaerobic oxidation of aromatic compounds and hydrocarbons," Curr Opin Chem Biol 6, 5 (2002) p. 604-611.

10. R. Charkraborty, J. D. Coates, "Anaerobic degradation of monoaromatic hydrocarbons," Appl Microbiol Biot 64, 4 (2004) p. 437-446.

11. R. U. Meckenstock, M. Safinowski, C. Griebler, "Anaerobic degradation of polycyclic aromatic hydrocarbons," FEMS Microbiol Ecol 49, 1 (2004) p. 27-36.

12. R. Rabus, "Biodegradation of hydrocarbons under anoxic conditions," in Petroleum Microbiology, eds. B. Ollivier and M. Magot (Washington: ASM Press, 2005), p. 277-299.

13. J. M. Suflita, I. A. Davidova, L. M. Gieg, M. Nanny, R. C. Prince, "Anaerobic hydrocarbon biodegradation and the prospects for microbial enhanced energy production." . Eds. , Elsevier BV: New York. (2004) pp. ." in Petroleum Biotechnology: Developments and Perspectives, eds. R. Vazquez-Duhalt and R. Quintero-Ramierez (New York: Elsevier BV, 2004), p. 283-305.

14. J. M. Suflita, M. J. McInerney, "Microbial approaches for the enhanced recovery of methane and oil from mature reservoirs," in Bioenergy, eds. J. D. Wall, C. S. Harwood and A. Demain (Washington: ASM Press, 2008), p. 389-403.

15. F. Widdel, R. Rabus, "Anaerobic biodegradation of saturated and aromatic hydrocarbons," Curr Opin Biotech 12, 3 (2001) p. 259-276.

16. R. Anderson, D. R. Lovley, "Hexadecane decay by methanogenesis," Nature 404 (2000) p. 722-723.

17. H. R. Beller, E. A. Edwards, "Anerobic toluene activiation by benzylsuccinate synthase in a highly enriched methanogenic culture," Appl Environ Microbiol 66, 12 (2000) p. 5503-5505.

18. E. A. Edwards, D. Grbic-Galic, "Anaerobicdegreadation of toluene and oxylene by a methanogenic consortium," Appl Environ Microbiol 60, 1 (1994) p. 313-322.

19. L. M. Gieg, K. E. Duncan, J. M. Suflita, "Bioenergy production via microbial conversion of residual oil to natural gas," Appl Environ Microbiol 74, 10 (2008) p. 3022-3029.

20. J. Kazumi, M. E. Caldwell, J. M. Suflita, D. R. Lovley, L. Y. Young, "Anaerobic degradation of benzene in diverse anoxic environments." Environ. Sci. Technol. 31 (1997): pp. 813-818.," Environ Sci Technol 31, 3 (1997) p. 813-818.

21. T. Siddique, P. M. Fedorak, J. M. Foght, "Biodegradation of short-chain n-alkanes in oil sands tailings under methanogenic conditions," Environ Sci Technol 40, 17 (2006) p. 5459-5464.

22. T. Siddique, P. M. Fedorak, M. D. MacKinnon, J. M. Foght, "Metabolism of BTEX and naphtha compounds to methane in oil sands tailings," Environ Sci Technol 41 (2007) p. 2350-2356.

23. G. T. Townsend, R. C. Prince, J. M. Suflita, "Anaerobic oxidation of crude oil hydrocarbons by the resident microorganisms of a contaminated anoxic aquifer," Environ Sci Technol 37, 22 (2003) p. 5213-5218.

24. G. T. Townsend, R. C. Prince, J. M. Suflita, "Anaerobic biodegradation of alicyclic constituents of gasoline and natural gas condensate by bacteria from an anoxic aquifer," FEMS Microbiol Ecol 49, 1 (2004) p. 129-135.

25. A. C. Ulrich, E. A. Edwards, "Physiological and molecular characterization of anaerobic benzene-degrading mixed cultures culture." Environ. Microbiol. 5, 2 (2003): pp. 92-102.," Environmetal Microbiology 5, 2 (2003) p. 92-102.

26. J. M. Weiner, D. R. Lovley, "Rapid benzene degradation in methanogenic sediments from a petroleum-contaminated aquifer," Appl Environ Microbiol 64, 5 (1998) p. 1937-1939.

27. K. Zengler, H. H. Ricknow, R. Rossello-Mora, W. Michaelis, F. Widdel, "Methane formation from long-chain alkanes by anaerobic microorganisms," Nature 401, 6750 (1999) p. 266-269.

28. C. J. McNamara, T. D. Perry, N. Wolf, R. Mitchell, R. Leard, J. Dante, "Corrosion of aluminum 2024 by jet fuel degrading microorganisms," CORROSION / 2003, Paper no. 03568 (Houston, TX: NACE International, 2003).

29. D. Lockridge, "New fuels, new problems," Heavy Duty Trucking, June (2007) p. 30-48.

30. K. L. Londry, J. M. Suflita, "Toxicity effects of organosulfur compounds on anaerobic microbial metabolism," Environ Toxicol Chem 17 (1998) p. 1199-1206.

31. F. A. Ali, N. Ghaloum, A. Hauser, "Structure representation of asphaltene GPC fractions from Kuwati residual oils," Energ Fuel 20, 1 (2006) p. 231-238.

32. G. Knothe, K. R. Steidley, "Lubricity of components of biodiesel and petrodiesel. The origin of biodiesel lubricity " Energ Fuel 19, 3 (2005) p. 1192-1200.

33. S. G. Fischer, L. S. Lerman, "Length-independent separation of DNA restriction fragments in two-dimensional gel electrophoresis," Cell 16, 1 (1979) p. 191-200.

34. Microbial Insights, Inc., "Denaturing gradient gel electrophoresis (DGGE)," [Website], www.microbe.com/ddge.html, (2004), [Accessed 2008 October 23].

35. J. R. Scully, "Polarization resistance method for determination of instantaneous corrosion rates," Corrosion 56, 2 (2000) p. 199-218.

36. J. R. Davis, ed., Metals Handbook, 2nd Ed. (Materials Park, OH: ASM International, 1998).

TABLES

Table 1. Chemical compositions of alloys in wt%.[36]

UNS	C	Mn	P	S	Si	Cr	Ni	N	Al	Cu	Fe	Mg	Zn
C10200	0.18-0.23	0.30-0.60	0.04	0.05							Bal.		
S30403		2.00	0.045	0.03	0.75	18.0-20.0	8.0-12.0	0.10			Bal.		
A95052		0.1			0.15	0.15-0.35			Bal.	0.1	0.4	2.2-2.28	0.1

Table 2. pH values of water layers after 6 month exposure to fuel and alloys.

	C10200	S30403 + A95052
ULSD	6.64	4.98
L100	3.41	3.49
B5	5.80	4.93
B20	4.64	5.21
B100	3.97	3.85

Initial distilled water pH = 5.75

Table 3. Fuel Specifications according to the U. S. Navy's F-76 limits.

Characteristic	ASTM Test Method	F-76 Limits	B 100	L100	ULSD
Acid Number	D 974	0.30 mg KOH/g max	0.26	1.95	0.03
Appearance @ 25 °C	D 4176	C&B	C & B	C & B / Red	C & B
Ash	D 482	0.005 wt. % max	0.002	0.002	<0.001
Carbon Residue (10% bottoms)	D 4530	0.14 wt. % max	0.67	0.62	0.02
Cetane Index	D 976	43 min	N/A	43	53
Cloud Point	D 5773	-1 deg C max	-1	-19	-13
Color max	D 1500	3 max	2	L 6.0	L 0.5
Corrosion @ 100 °C	D 130	1 max	1a	1a	1a
Demulsification @ 25 °C	D 1401	10 minutes max	26	5	2
Density @ 15 °C	D 4052	876 kg/m^3 max	886	863	829
Distillation	D 86				
Initial Boiling Point		deg C Report	N/A	119	202
10% Point		deg C Report	N/A	168	227
50% Point		deg C Report	N/A	265	262
90% Point		357 deg C max	N/A	325	318
End Point		385 deg C max	N/A	344	356
Residue		vol. % max	N/A	2	2
Loss		vol. % max	N/A	0	0
Flash Point	D 93	60 deg C min	158	36	<30
Hydrogen Content	D 7171	12.5 wt. % max	11.8	12.2	13.8
Particulates	D 6217	10 mg/L max	28	4	1
Pour Point	D 5949	-6 deg C max	-3	-36	-18
Storage Stability	D 5304	3.0 mg/100 mL max	27.8	37.5	0.4
Trace Metals - Calcium	D 7111	1.0 ppm max	4.5	<0.1	<0.1
Trace Metals - Lead	D 7111	0.5 ppm max	0.2	<0.1	<0.1
Trace Metals - Sodium + Potassium	D 7111	1.0 ppm max	<0.1	0.9	0.4
Trace Metals - Vanadium	D 7111	0.5 ppm max	<0.1	<0.1	<0.1
Sulfur Content by UV	D 5453	10,000 ppm max	3	1,273	2
Viscosity @ 40 °C	D 445	1.7-4.3 cSt	4.1	2.3	2.8
Sediment and Water by Centrifuge	D 2709	0.05 vol % max	0	0	0

Additional Non-Specification Tests for Informational Purposes Only

Aromatics by HPLC	D 6591				
Mono-Aromatics		mass %	0	45	20
Di-Aromatics		mass %	0	4	1
Total Aromatics		mass %	0	49	21
Diesel MSEP	D 7261		0	0	42
Filtration Time	In-House	min/gal	1463	118	59

Table 4. Bacterial and fungal populations of water layers exposed for 2 weeks to pre-exposure fuels. Identification numbers (#) in the tables correspond to number displayed on the band patterns.

Fuel	Bacteria	#	Fungi	#
B100	(Uncultured)	1.1	*Cryptococcus*	1.1F
	Sphingomonas spp.	1.2	*Aureobasidium*	1.2F
	Methylobacter / Methylobacterium spp.	1.3		
L100	*Bacillus spp.*	2.1		
	Thermomonas	2.3		
Inoculum	*Niastella*	3.1	*Rhodotorula*	3.1F
	Acinetobacter spp.	3.2	*Mycosphaerella*	3.2F
	Bacillus spp.	3.3		
ULSD	*Sphingomonas spp.*	4.1	*Paecilomyces spp.*	4.1F
	Chelatococcus spp.	4.2		
	Bradyrhizobium spp.	4.3		

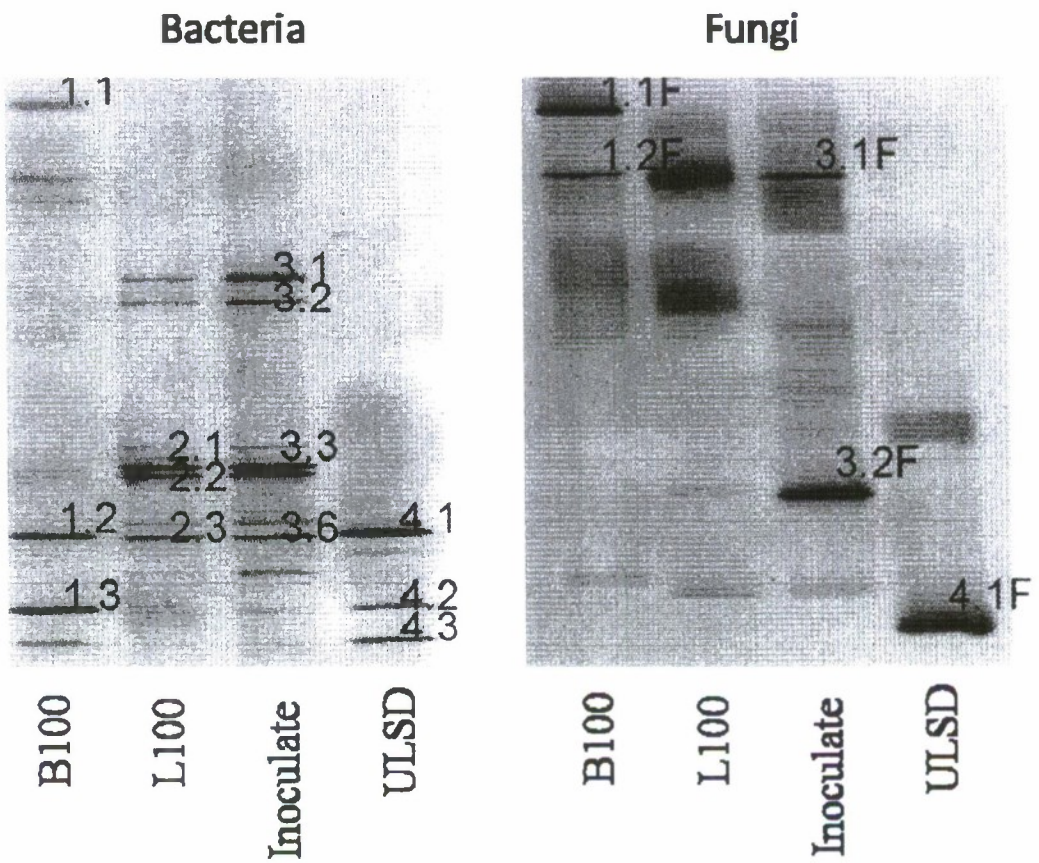

Table 5. Bacterial and fungal populations of water layers exposed for 6 months to different fuels/alloy combinations. Alloys S30403 and A95052 were exposed in the same container. Identification numbers (#) in the tables correspond to number displayed on the band patterns.

Alloy(s)	Fuel	Bacteria	#	Fungi	#
C10200	ULSD	*Sphingomonas spp* (Uncultured)	1.1 1.2	*Aureobasidium* (Uncultured)	1.1F 1.2F
	B5	*Sphingomonas spp* *Alphaproteobacteria* *Sphingomonadaceae* *Sphingomonadaceae*	2.1 2.2 2.3 2.4	*Calosphaeria*	2.1F
	B20	(Uncultured) (Uncultured) *Alphaproteobacteria*	3.1 3.2 3.3	*Rhodotorula* (from Inoculum)	3.1F
	B100			*Aureobasidium*	4.1F
	L100			*Saccharomyces* *Cladosporium*	5.1F 5.2F
S30403 **A95052**	ULSD	(Uncultured) (Uncultured) (Uncultured)	6.1 6.2 6.3	(Uncultured)	6.1F
	B5	*Sphingomonas spp* *Alphaproteobacteria* *Betaproteobacterium*	7.1 7.2 7.3 7.4	*Paecilomyces spp.*	7.1F
	B20	*Sphingomonas spp* *Alphaproteobacteria* *Alphaproteobacteria*	8.1 8.2 8.3	(Uncultured)	8.1F
	B100			*Paecilomyces spp.*	9.1F
	L100				

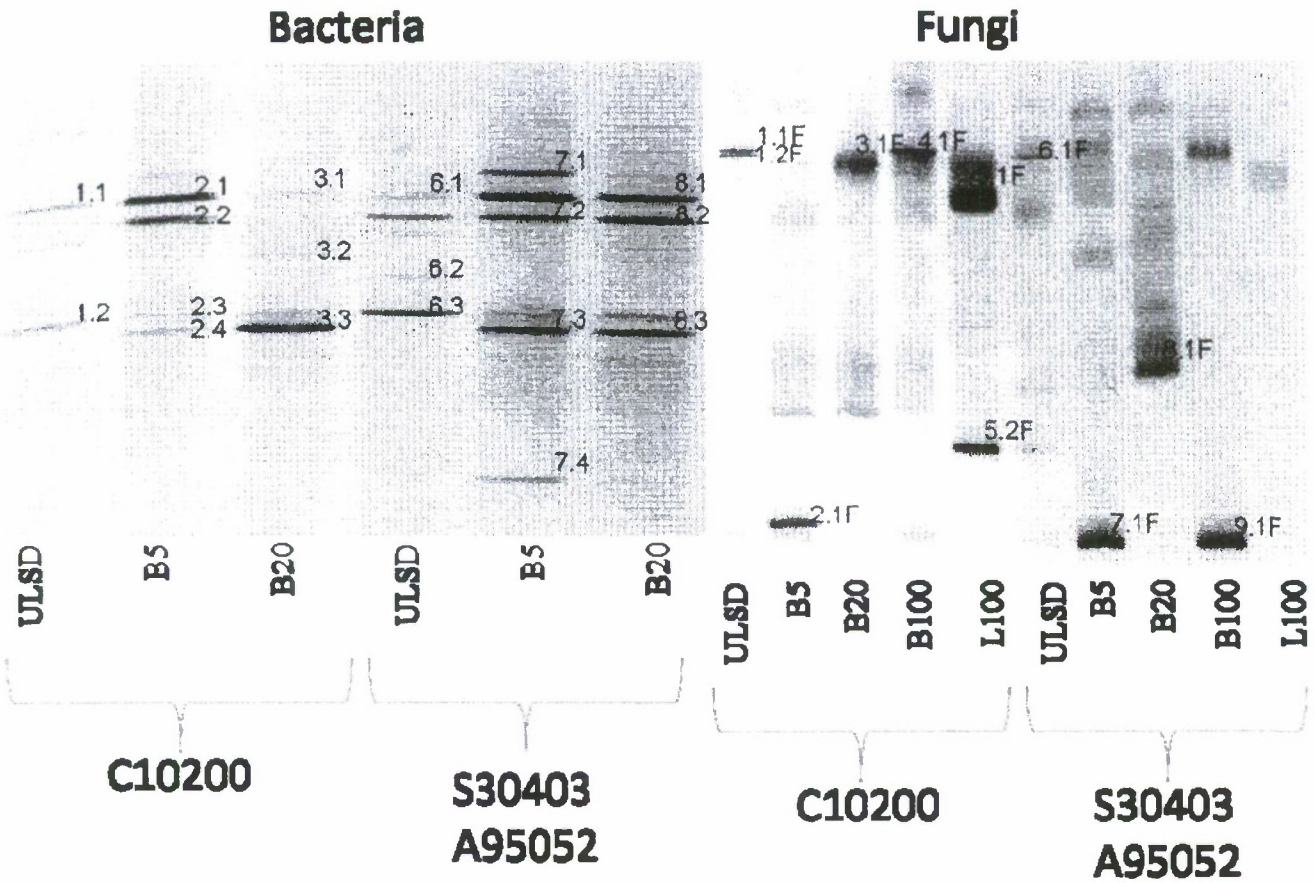

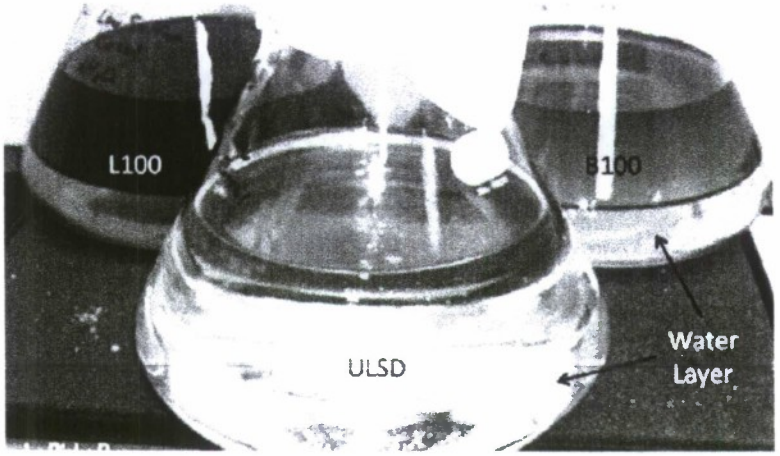

Figure 1. Image of the pre-exposure fuels L100, ULSD, and B100 and distilled water layers.

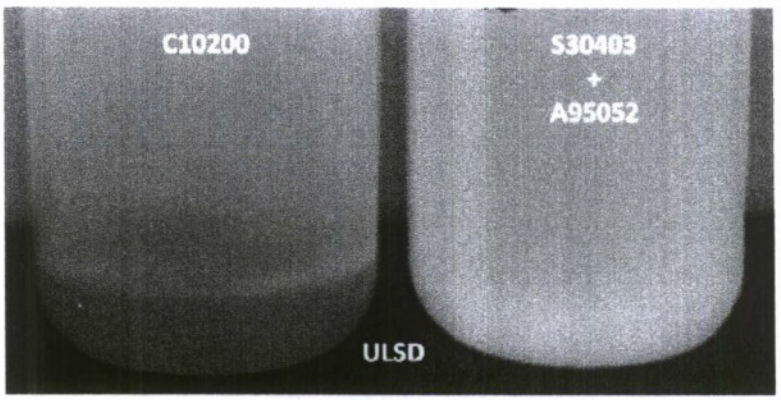

Figure 2. ULSD fuel after 6 month exposure to C10200 and S30403+A95052 and distilled water. The water layer was removed and orange corrosion products collected at the bottom of the fuel exposed to C10200.

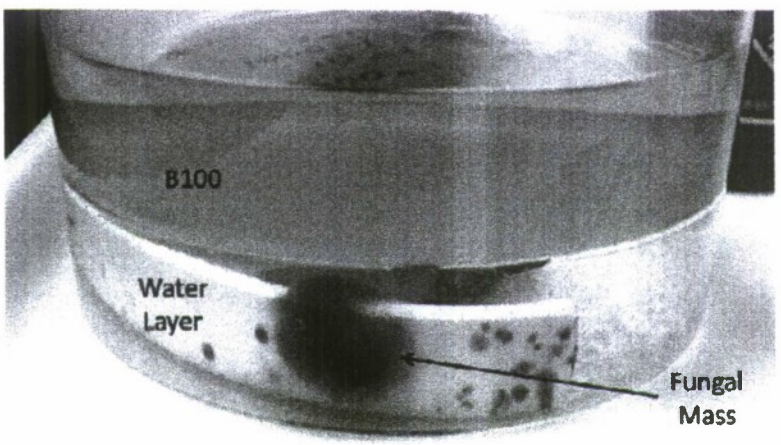

Figure 3. Illustration of the observed biofouling (fungal mass) in the water layer exposed to B100 for 6 months. In addition, the color change of the B100 from yellow (Figure 1) to the bright green can also be seen.

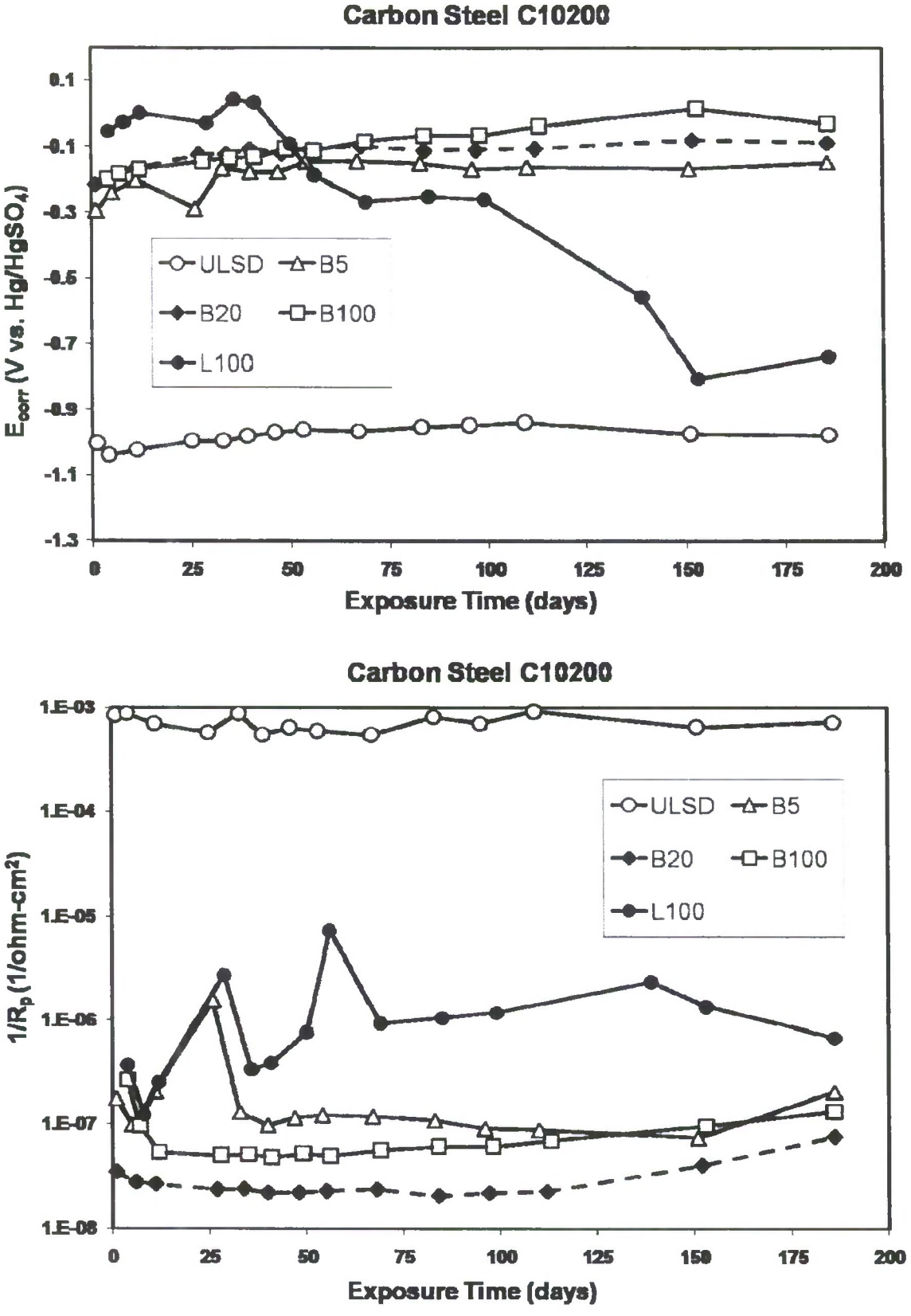

Figure 4. E_{corr} ($V_{Hg/HgSO4}$) and $1/R_p$ (instantaneous corrosion rate) trends for carbon steel C10200 exposed to each of the 5 fuel/water mixtures.

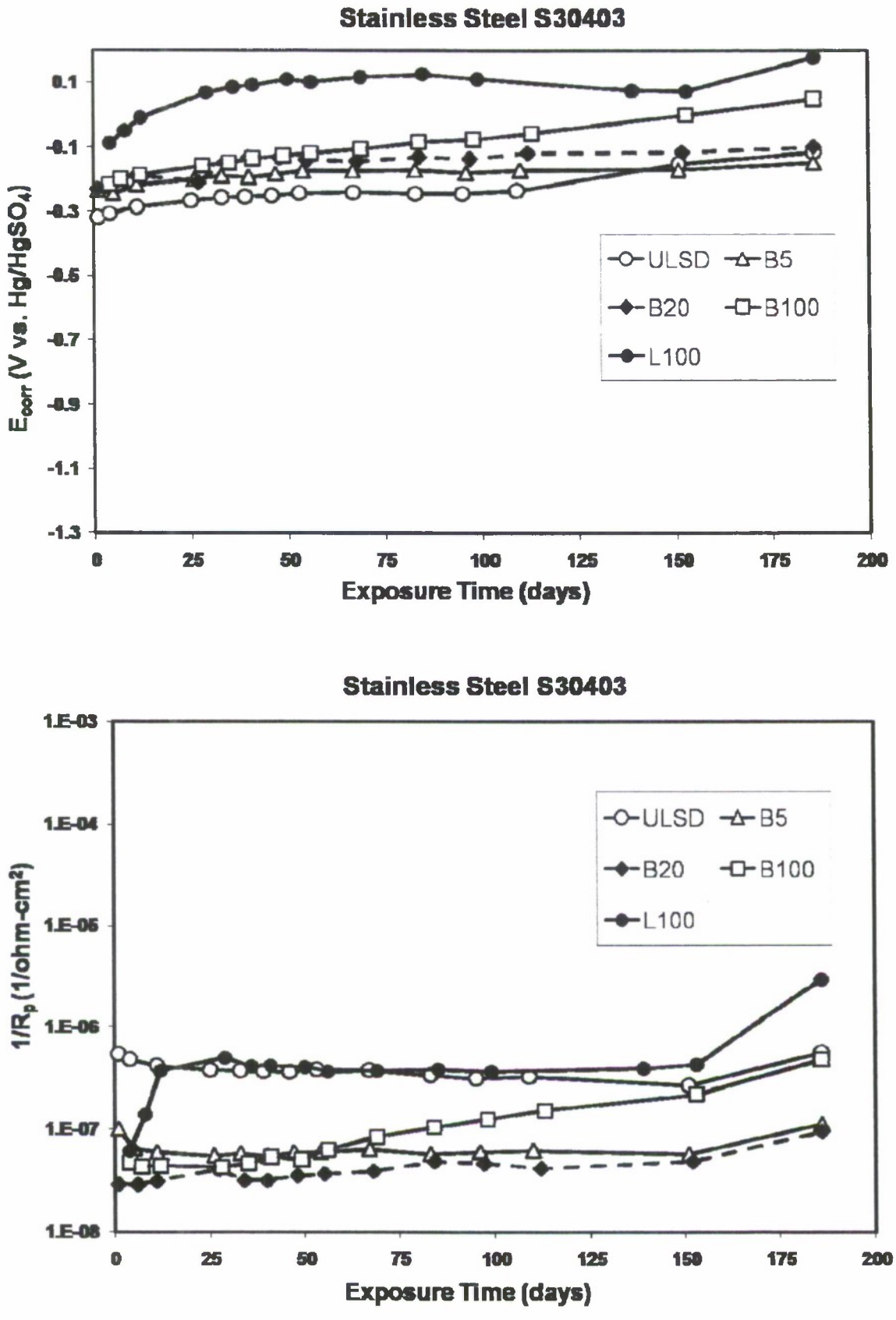

Figure 5. E_{corr} ($V_{Hg/HgSO4}$) and $1/R_p$ (instantaneous corrosion rate) trends for stainless steel S30403 exposed to each of the 5 fuel/water mixtures.

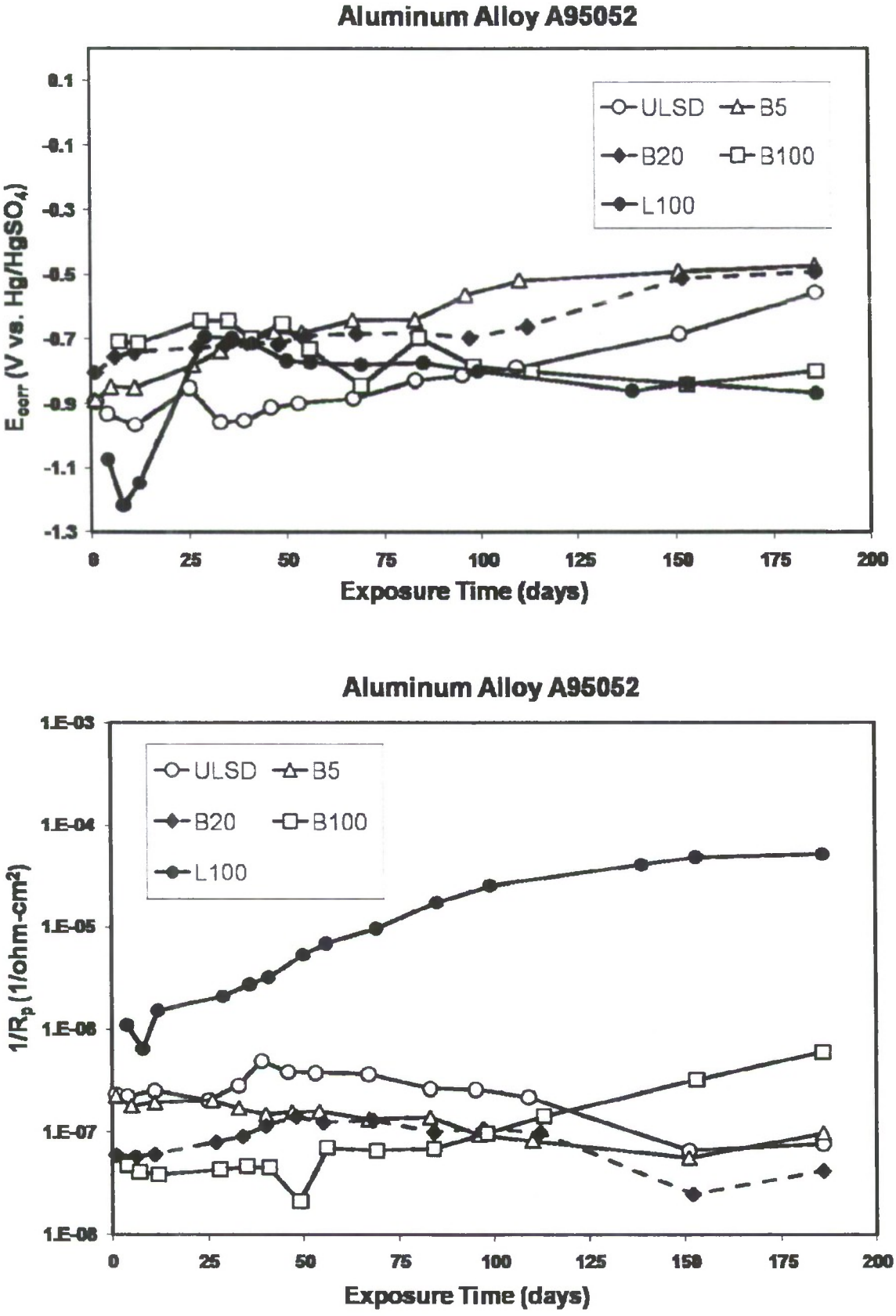

Figure 6. E_{corr} ($V_{Hg/HgSO4}$) and $1/R_p$ (instantaneous corrosion rate) trends for aluminum alloy A95052 exposed to each of the 5 fuel/water mixtures.

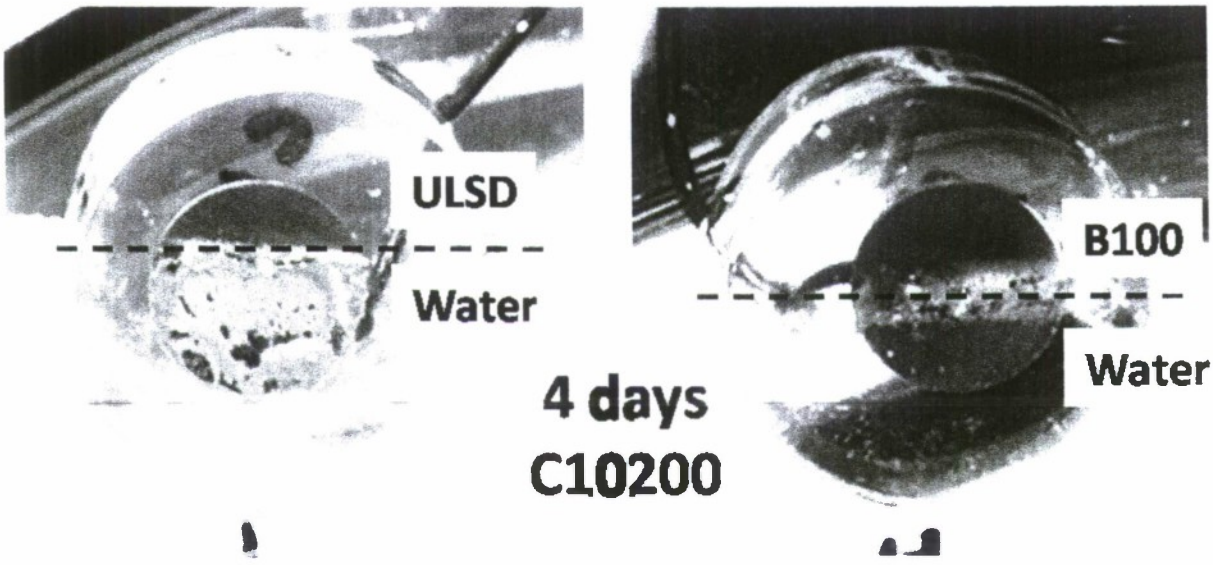

Figure 7. Carbon steel C10200 after 4 days of exposure to distilled water mixed with ULSD and B100 in a 1:1 ratio. In the ULSD exposure, corrosion products were visible on the metal surface exposed to the water layer but not in the fuel layer. For exposure to B100, only a discoloration was observed at the fuel/water interface. No corrosion was observed even on the surface exposed to the water layer when B100 was present.

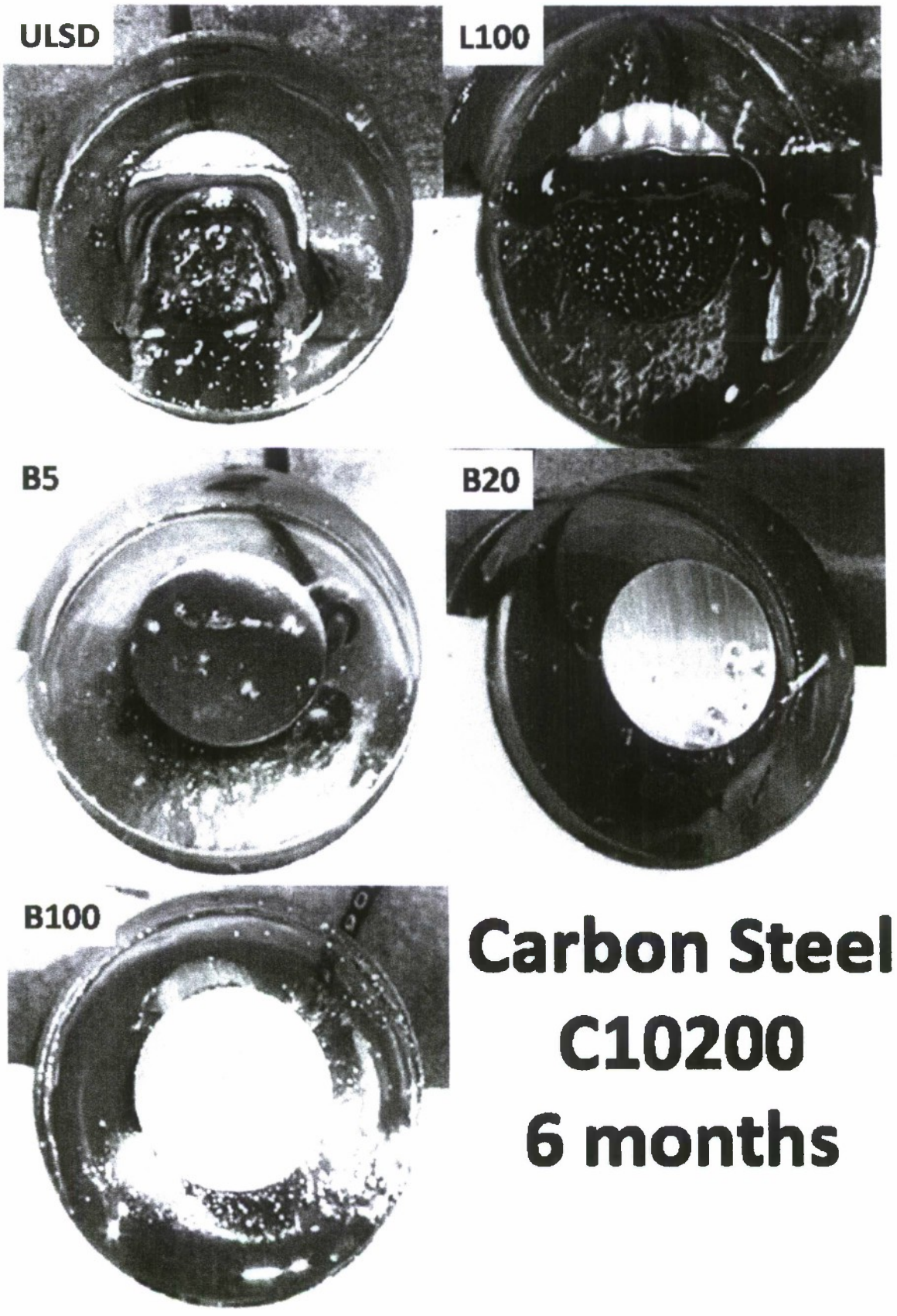

Figure 8. Images of carbon steel C10200 exposed to the five different fuel/water mixtures for six months.

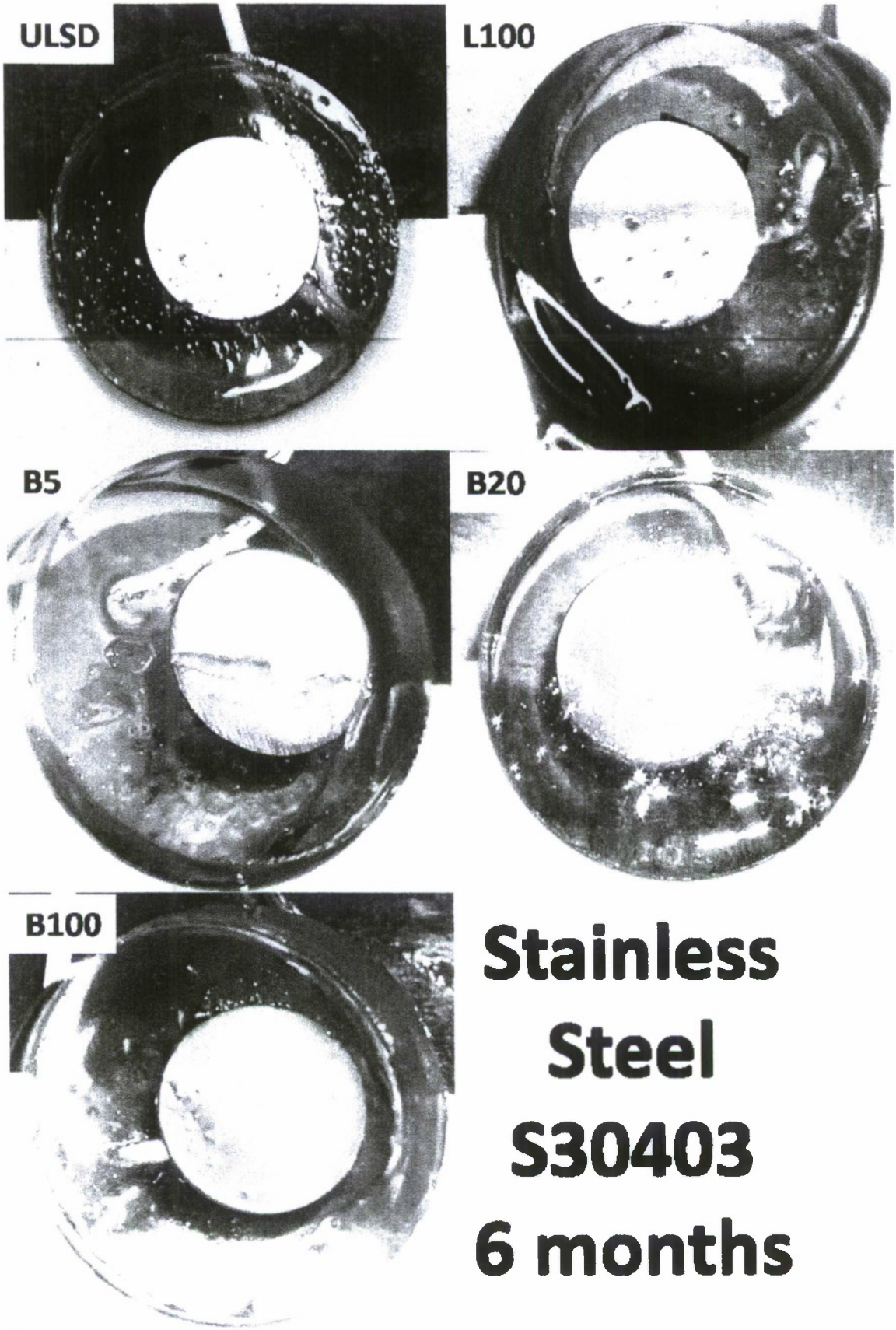

Figure 9. Images of stainless steel S30403 coupons exposed to the five different fuel/water mixtures for 6 months.

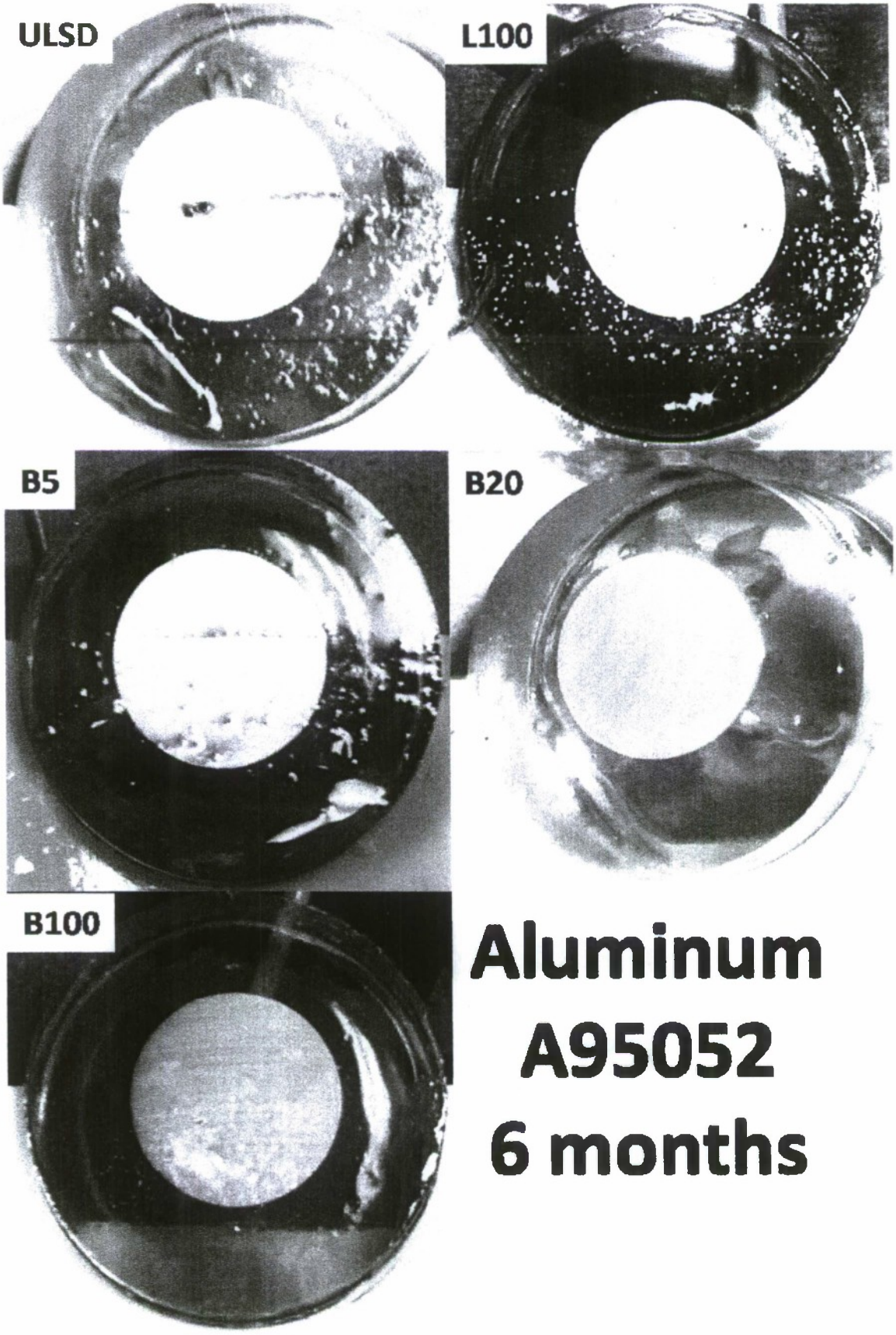

Figure 10. Images of aluminum alloy A95052 coupons exposed to the five different fuel/water mixtures for 6 months.